09

Synthesis and Luminescence of Ba_2YCl_7

© R.A. Bhoyar[1], Y.K. More[2], S.P. Wankhede[3], P.D. Belsare[4], S.V. Moharil[5]

[1] RTM Nagpur University,
440033 Nagpur, India
[2] Department of Physics, Bhiwapur Mahavidyalaya,
441201 Bhiwapur, India
[3] Department of Physics, K.D.K. College of Engineering,
Nagpur, India
[4] Shri Ramdeobaba College of Engineering and Management,
440013 Nagpur, India
[5] Department of Physics, RTM Nagpur University,
440033 Nagpur, India

E-mail: rajanibhoyar1@gmail.com

Received February 28, 2024
Revised March 24, 2024
Accepted March 24, 2024

New findings for Ba_2YCl_7 activated with 4f transition elements Eu^{2+} and Ce^{3+} are presented. These phosphors were synthesized using wet chemical procedure. As-synthesized Ce^{3+}-doped sample exhibited intense photoluminescence (PL). For Eu^{2+} activation, further heat treatment in reducing atmosphere at 700°C was necessary. Intense emission from these activators could be identified with the allowed intra-configurational transitions. Ease of preparation combined with intense PL make these hitherto unexplored phosphors potential candidates for applications such as scintillation.

Keywords: halide, photoluminescence, phosphor.

DOI: 10.61011/PSS.2024.04.58210.1

1. Introduction

Fam Ngok T'en and Morozov studied the phase diagram of the system $BaCl_2-YCl_3$ [1]. Later, in this system compound Ba_2YCl_7 was first described by Blachnik *et al.* [2]. Detailed structure was described by Wickleder *et al.* [3] who also found that solid solutions between Ba_2YCl_7 and Ba_2ErCl_7 exhibit intense up-conversion luminescence in various spectral regions. Mechanism of Er^{3+} up-conversion was investigated by Burlot-Loison *et al.* [4]. Karbowiak *et al.* reported luminescence of U^{3+} [5] and U^{4+} [6] in this host. Karbowiak *et al.* [7] also analysed energy levels of lanthanide activators in Ba_2YCl_7 lattice. From theoretical consideration, Canning *et al.* predicted it to be a good scintillator [8].

On this background, it is quite surprising to note that luminescence of known efficient activators like Ce^{3+} or Eu^{2+} has not been explored in Ba_2YCl_7 lattice. Due to the presence of divalent Ba^{2+} and trivalent Y^{3+}, variety of activators can be accommodated in Ba_2YCl_7 lattice. For the same reason, this host could also be ideal for studying energy transfers between heterovalent ions. Luminescence of both Ce^{3+} and Eu^{2+} originates in the transitions between the lowest energy levels of $4f^N$ configuration and the higher states resulting from promoting of one electron to d shell. These transitions have allowed nature and thus appreciable oscillator strength. Usually, strong luminescence originating in the allowed transitions is expected for Ce^{3+} [9,10] as well as Eu^{2+} [11] ions which have been studied in numerous hosts.

We have now studied luminescence of $Ba_2YCl_7:Ce^{3+}$ and $Ba_2YCl_7:Eu^{2+}$. These phosphors exhibited efficient luminescence. Outcome of these studies are described and discussed in this article.

2. Experimental

Detailed description of the experimental procedures was given in our earlier article [12]. Essentials are reproduced here in short. Wet chemical synthesis was used to prepare the phosphors. Ingredient compounds of barium ($BaCl_2$) and scandium (Sc_2O_3) were obtained in liquid form by using HCl as a solvent. For doping Eu_2O_3 or cerium oxalate were likewise dissolved in HCl. These solutions were poured in a single beaker which was placed on a hot plate. The temperature was raised till the acid started boiling. The heating was continued till the all the solvent got evaporated. The resulting solid mass was removed and heated in a crucible, at 475 K for 2 hours in air and then cooled to room temperature. Finally, the prepared phosphors were crushed and sieved to yield particles smaller than 72 μm. Eu^{2+} doping was attained by heating the as-prepared phosphors in a crucible closed with a lid. The temperature was varied between 675–975 K. Charcoal was burned to generate reducing conditions. The phosphor powders so obtained were sandwiched between two silica slides which

were placed in a cell inside a spectro-fluorimeter. Hitachi F-7000 spectro-fluorimeter was used for photoluminescence measurements over a range of 220−700 nm. Spectral slit widths were chosen as 1 nm to get good resolution. The same instrument enabled recording of reflectance spectra. $BaSO_4$ was used as a reference. Powder diffraction patterns were obtained on XPERT-PRO diffractometer. CuK_α ($\lambda = 1.54059$ Å) radiation was used. These measurements ensured compound formation. Luminescence decay was studied with the help of Horiba Fluorimax 3 spectro-fluorimeter using TCSPC software. Horiba 250-nm/300-nm nano LEDs were used as excitation source.

3. Results and discussion

For confirmation of the phase formation, diffraction pattern for Ba_2YCl_7 was recorded (Figure 1, *a*). Rietveld analysis was carried out using Fullprof software. These results are also included in Figure 1, *b*.

Goodness-of-Fit parameters are $\chi^2 = 6.83$, profile residual $R_p = 8.51$, and weighted profile residual $R_{wp} = 1.32$. The observed pattern was refined to monoclinic system in the space group $P2_1/c$. The unit cell dimensions are $a = 6.7940$, $b = 15.5250$ and $c = 10.4960$ Å, $V = 1107.0358$ Å^3. These are consistent with the published

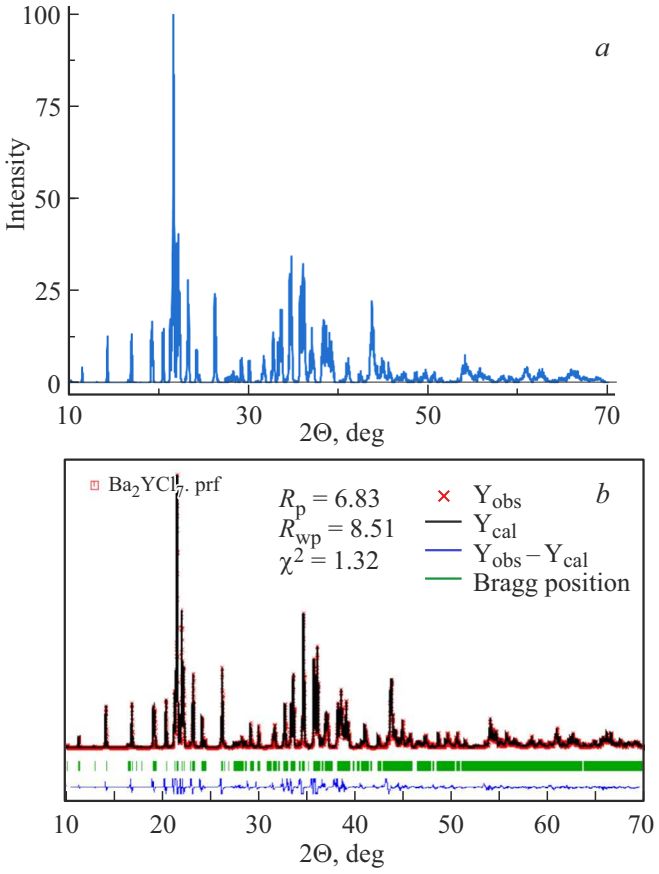

Figure 1. *a*) X-ray diffraction patterns of Ba_2YCl_7; *b*) Rietveld refinement.

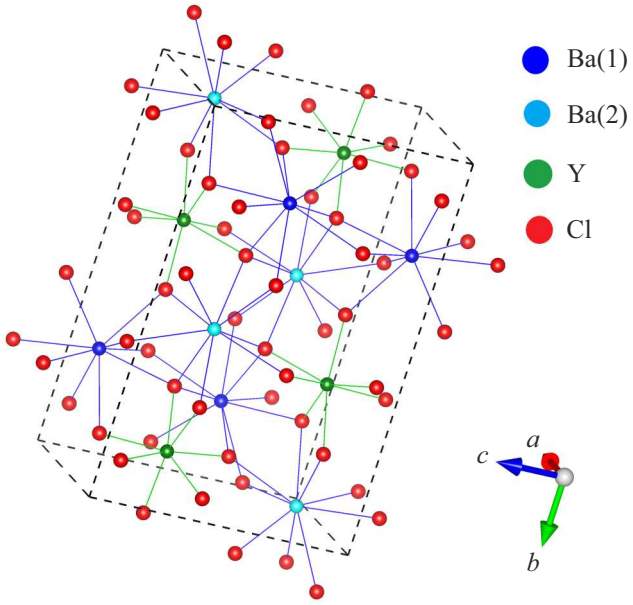

Figure 2. Unit cell of Ba_2YCl_7 showing 7-coordinated Y and 9-coordinated Ba(1) and Ba(2).

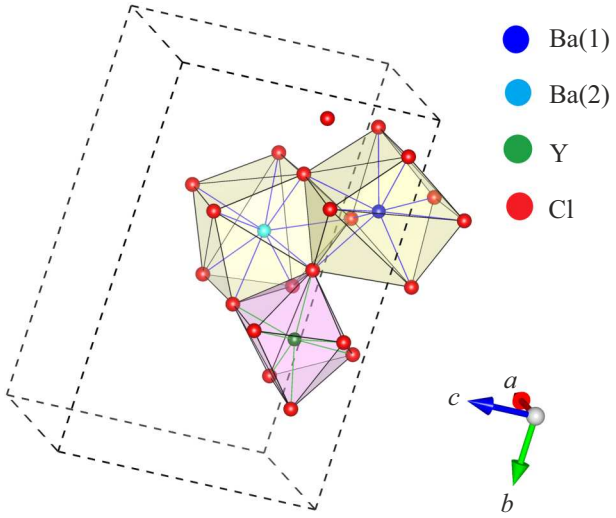

Figure 3. Coordination polyhedra of Ba_2YCl_7. $[Ba(1)Cl_9]$ polyhedra are linked via opposite edges to form chains according to $[Ba(1)Cl_4/2Cl_5]$ running along the *c* axis. The $[Ba(2)Cl_9]$ polyhedra build up zig-zag chains along the *a* axis. YCl_7 polyhedra are in the form of a trigonal prism and capped on one rectangular face.

data [3]. In Ba_2YCl_7 structure, Y^{3+} ions occupy only one type of site and are coordinated with 7 chlorine ions. In contrast, Ba^{2+} ions occupy two crystallographically different sites. These are denoted as Ba(1) and Ba(2). At both these positions, these are surrounded by 9 chlorine ions (Figure 2).

Two positions differ in orientations. The $[Ba(1)Cl_9]$ polyhedra form chains parallel to *c* axis. Whereas the $[Ba(2)Cl_9]$ polyhedra form criss-cross chains in the direction

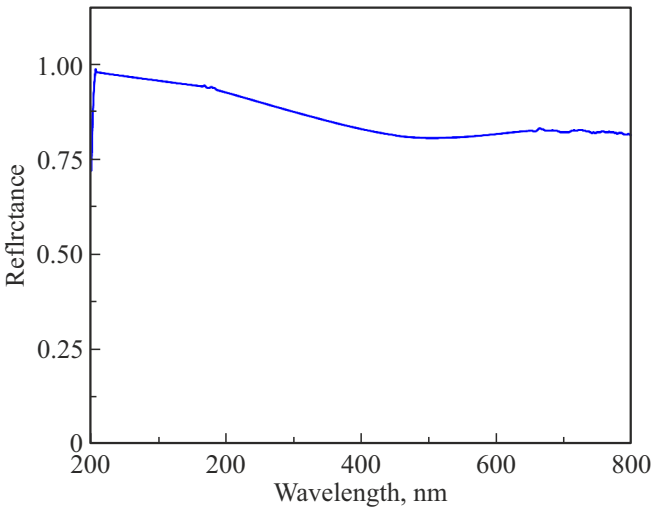

Figure 4. Reflectance spectrum of Ba_2YCl_7.

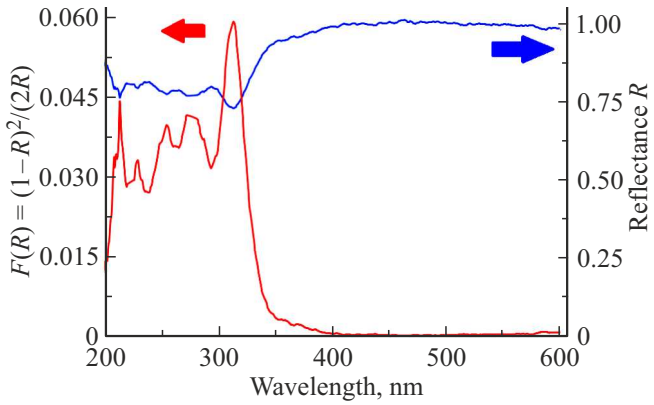

Figure 5. Reflectance spectrum of $Ba_2YCl_7:Ce^{3+}$ (2 mol.%).

of *a* axis. The structure is completed by linking these chains by sharing triangular faces. YCl_7 polyhedra are of trigonal prism shape. These are placed on a rectangular face (Figure 3). Y^{3+} polyhedra appear somewhat distorted imparting C_1 surroundings. $Y^{3+}-Y^{3+}$ separations are large, of the order of 6.5 Å, thus making YCl_7 polyhedra isolated. The Y−Cl bond lengths around 2.7 Å are usual as found in complex chloride compounds of yttrium.

Figure 4 shows reflectance spectrum for Ba_2YCl_7. No absorption attributable to a transition across the band gap can be observed. Thus, the band gap is less than 6 eV. On the other hand, Canning *et al.* [8] estimated the band gap as low as 4.7 eV. In the theoretical calculations like DFT, band gaps are often underestimated.

Introduction of lanthanide ions lead to absorption within the band gap. Figure 5 shows reflectance spectrum for $Ba_2YCl_7:Ce^{3+}$. Absorption bands around 213, 228, 256, 280, and 314 nm can be seen. This is consistent with expected 5-fold splitting of Ce^{3+} energy levels in C_1 symmetry.

Similar results for $Ba_2YCl_7:Eu^{2+}$ are presented in Figure 6. A strong absorption band around 285 nm with several shoulders, on long as well as short wavelength sides are observed. These are characteristic of Eu^{2+}.

Ce^{3+} ions are expected to enter 7-coordinated yttrium sites. As-prepared samples exhibited intense photoluminescence (PL) (Figure 7).

A typical split peak with double maxima at 340 and 358 nm can be seen. The corresponding excitation spectra show the most intense peak around 312 nm and distinct shoulders around 245 and 280 nm. The spectra can be attributed to transitions between split ground state $^2F_{5/2}$, $^2F_{7/2}$, of $4f^1$ configuration and the excited states belonging to $4f^05d^1$ configuration. From these data, we obtain doublet splitting 1478 cm^{-1}, Stokes shift $\Delta s = 2639\,cm^{-1}$ and „crystal field splitting“ 8675 cm^{-1}. The Δs is close to 2200 cm^{-1}, which is „the most frequently observed“ number [9]. Effect of concentration is also shown in Figure 2. Maximum PL intensity is observed for 1 mol.%.

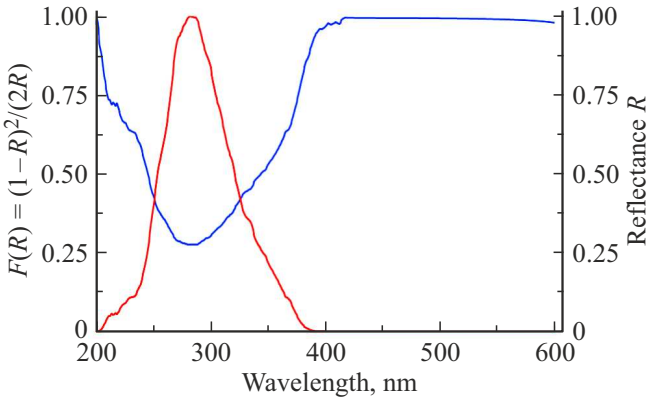

Figure 6. Reflectance spectrum of $Ba_2YCl_7:Eu^{2+}$ (2 mol.%).

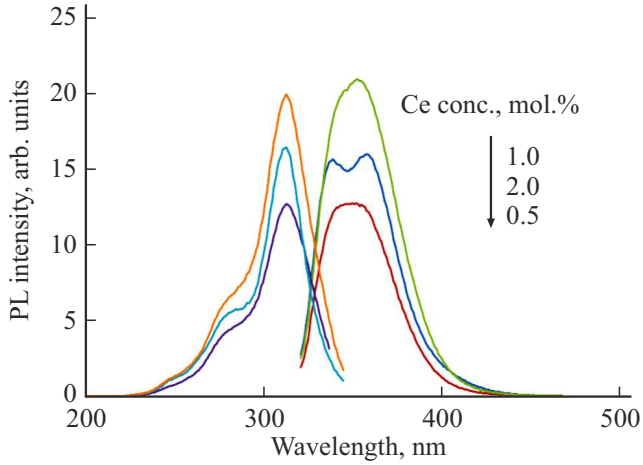

Figure 7. PL and PL emission spectra for $Ba_2YCl_7:Ce^{3+}$. Emission spectra were obtained using 312-nm excitation. Excitation spectra were recorded by monitoring 358-nm emission.

From PL spectra of Ce^{3+}, those for Eu^{2+} can be estimated using empirical relations given by Dorenbos [13].

$$E(7, 2+, A) = (0.64 \pm 0.02)E(1, 3+, A) + (0.53 \pm 0.06)\,\text{eV},$$

where $E(7, 2+, A)$ are positions of Eu^{2+} excitation/emission and $E(1, 3+, A)$ are the corresponding positions for Ce^{3+}. The equation holds good when the Ce^{3+} and Eu^{2+} are at the same type of site. In the context of this work, owing to isovalency Eu^{2+} may be assumed to be located at Ba^{2+} site. Ce^{3+} can replace Y^{3+}, but considering the ionic sizes it may also be found at Ba^{2+} site. If latter is the case and the charge compensating defect is away, then the above equation can be applied.

Substituting data for Ce^{3+} in the right-hand side, Eu^{2+} emission is expected to be around 425–442 nm.

Figure 8 shows the PL spectra for $Ba_2YCl_7:Eu^{2+}$ (2 mol.%). An intense emission in form of a band around 385 nm is seen. As this value differs considerably from

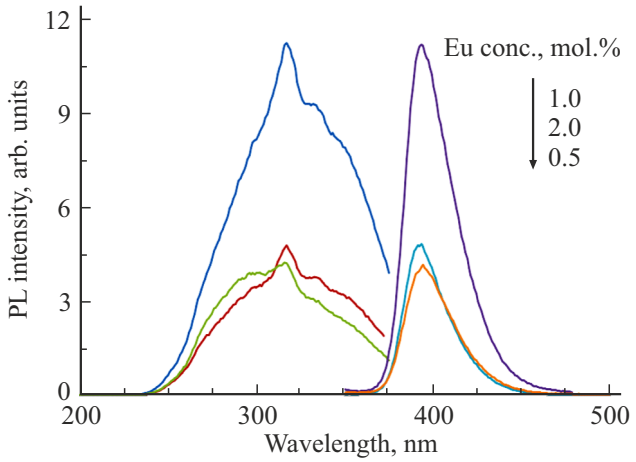

Figure 8. PL and PL emission spectra for $Ba_2YCl_7:Eu^{2+}$. Emission spectra were obtained using 320-nm excitation. Excitation spectra were recorded by monitoring 385-nm emission.

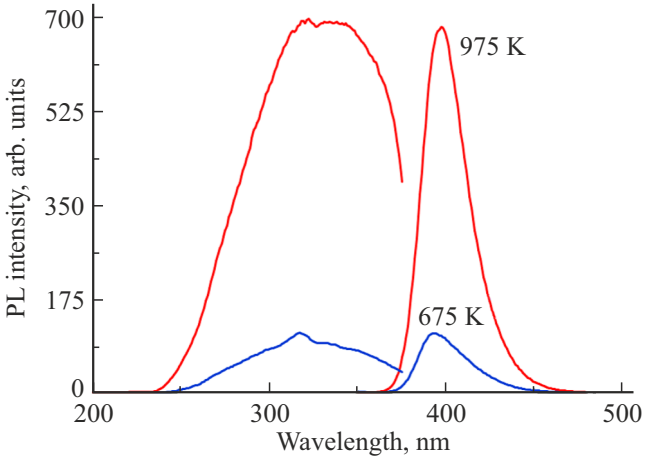

Figure 9. Effect of reduction temperature on the PL intensity of $Ba_2YCl_7:Eu^{2+}$.

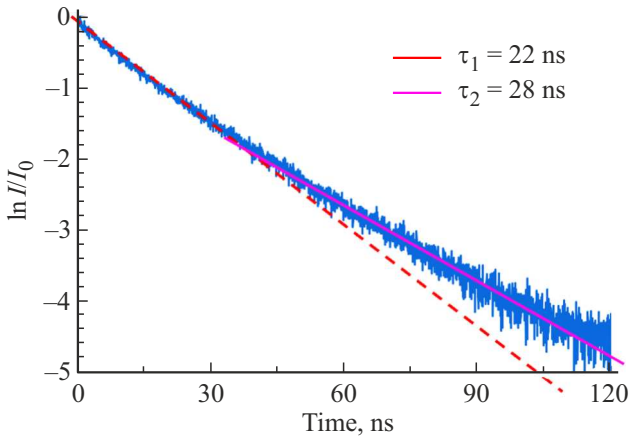

Figure 10. Luminescence intensity decay for $Ba_2YCl_7:Ce^{3+}$ (1.0 mol.%). Decay was monitored for 358-nm emission and 250-nm excitation.

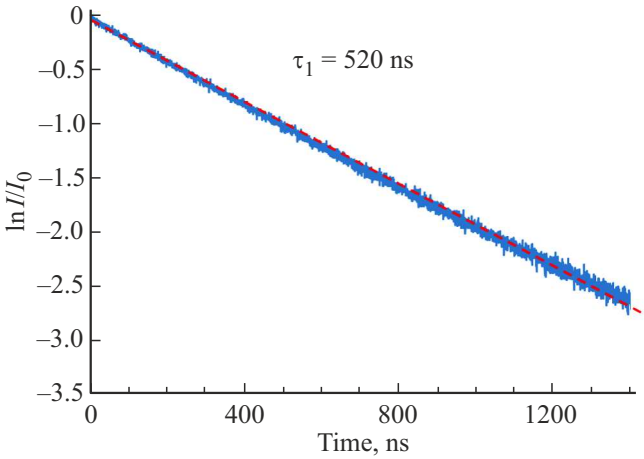

Figure 11. Luminescence intensity decay for $Ba_2YCl_7:Eu^{2+}$ (2.0 mol.%). Decay was monitored for 385-nm emission and 300-nm excitation.

that predicted above, it can be concluded that Eu and Ce are not at the same sites. Thus, Eu is at Ba site while Ce at Y. Effect of Eu concentration is also shown in Figure 8. No concentration quenching was observed up to 2 mol.%.

Dependence of PL intensity on the reduction temperature is shown in Figure 9. Though Eu^{2+} emission is observed at the reduction temperature of 675 K, intensity increases manifold when the reduction is carried out at 975 K. The excitation spectrum consists of broad unresolved bands, the one with the highest intensity is having a peak at 320 nm.

Lifetime is another important parameter which can reflect on the utility of a phosphor for given application. For example, for a scintillation detector short lifetimes are desirable. Accordingly, luminescence decay was studied for both phosphors. Lifetime measurements results for Ce-doped samples are shown in Figure 10, where I_0 is the initial intensity and I is the intensity at time t.

The decay is not exponential but two components with lifetimes $\tau_1 = 22$ and $\tau_2 = 28$ ns can be distinguished. The decay is fast enough to be of use in scintillation applications. Similar results for Eu-doped samples are plotted in Figure 11. Eu^{2+} decay is exponential with lifetime τ of 520 ns.

4. Conclusions

Intense emission is observed in for $Ba_2YCl_7:Ce^{3+}$ (1.0 mol.) and $Ba_2YCl_7:Eu^{2+}$ (2.0 mol.%). Both phosphors emit in near ultraviolet region. Ce^{3+} emission is quenched above 1 mol.% while that of Eu^{2+} showed no concentration quenching up to 2.0 mol.%. Ce^{3+} is incorporated at yttrium site while Eu^{2+} is accommodated at Ba sites. The luminescence is characterized by fast decay time being 22 ns for Ce^{3+} and 590 ns for Eu^{2+}. These features make the phosphors potential candidates for use as scintillation detectors. Presence of Ba in the host ensures good absorption of X-rays in radiology range and thus these phosphors can be useful for X-ray imaging.

Conflicts of interest

The authors declare that they have no conflict of interest.

References

[1] Fam Ngok T'en, I.S. Morozov. Russ. J. Inorg. Chem. **14**, *Part 1*, 713 (1969).
[2] R. Blachnik, J.E. Alberts. Z. Anorg. Allg. Chem. **490**, *1*, 235 (1982).
[3] M.S. Wickleder, P. Egger, T. Riedener, N. Furer, H.U. Güdel, J. Hulliger. Chem. Mater. **8**, *12*, 2828 (1996).
[4] R. Burlot-Loison, M. Pollnau, K. Krämer, P. Egger, J. Hulliger, H.U. Güdel. J. Opt. Soc. Am. B **17**, *12*, 2055 (2000).
[5] M. Karbowiak, A. Mech, J. Drożdżyński, Z. Gajek, N.M. Edelstein. New J. Chem. **26**, *11*, 1651 (2002).
[6] M. Karbowiak, A. Mech, J. Drożdżyński, N.M. Edelstein. Phys. Rev B **67**, *19*, 195108 (2003).
[7] M. Karbowiak, J. Cichos, C. Rudowicz. J. Phys. Chem. A **116**, *43*, 10574 (2012).
[8] A. Canning, A. Chaudhry, L.-W. Wang, R. Boutchko, S.E. Derenzo, M.J. Weber. 2007 IEEE Nuclear Sci. Symposium Conf. Record, 2466 (2007).
[9] P. Dorenbos. J. Lumin. **91**, *3–4*, 155 (2000).
[10] P. Dorenbos. Phys. Rev. B **62**, *23*, 15650 (2000).
[11] P. Dorenbos. J. Lumin. **104**, *4*, 239 (2003).
[12] D.H. Gahane, N.S. Kokode, P.L. Muthal, S.M. Dhopte, S.V. Moharil. Opt. Mater. **32**, *1*, 18 (2009).
[13] P. Dorenbos. J. Phys. C: Condens. Matter **15**, *27*, 4797 (2003).